Human Genetics (2023) 142:1755–1776
https://doi.org/10.1007/s00439-023-02613-6

ORIGINAL INVESTIGATION

Phenotypic correlates of structural and functional protein impairments resultant from *ALDH5A1* variants

Itay Tokatly Latzer[1,2] · Jean-Baptiste Roullet[3] · Samuele Cesaro[4] · Melissa L. DiBacco[1] · Erland Arning[5] · Alexander Rotenberg[1,6] · Henry H. C. Lee[6,7] · Thomas Opladen[8] · Kathrin Jeltsch[8] · Àngels García-Cazorla[9] · Natalia Juliá-Palacios[9] · K. Michael Gibson[3] · Mariarita Bertoldi[4] · Phillip L. Pearl[1]

Received: 26 June 2023 / Accepted: 27 October 2023 / Published online: 14 November 2023

Abstract

To investigate the genotype-to-protein-to-phenotype correlations of succinic semialdehyde dehydrogenase deficiency (SSADHD), an inherited metabolic disorder of γ-aminobutyric acid catabolism. Bioinformatics and in silico mutagenesis analyses of *ALDH5A1* variants were performed to evaluate their impact on protein stability, active site and co-factor binding domains, splicing, and homotetramer formation. Protein abnormalities were then correlated with a validated disease-specific clinical severity score and neurological, neuropsychological, biochemical, neuroimaging, and neurophysiological metrics. A total of 58 individuals (1:1 male/female ratio) were affected by 32 *ALDH5A1* pathogenic variants, eight of which were novel. Compared to individuals with single homotetrameric or multiple homo and heterotetrameric proteins, those predicted not to synthesize any functional enzyme protein had significantly lower expression of *ALDH5A1* ($p = 0.001$), worse overall clinical outcomes ($p = 0.008$) and specifically more severe cognitive deficits ($p = 0.01$), epilepsy ($p = 0.04$) and psychiatric morbidity ($p = 0.04$). Compared to individuals with predictions of having no protein or a protein impaired in catalytic functions, subjects whose proteins were predicted to be impaired in stability, folding, or oligomerization had a better overall clinical outcome ($p = 0.02$) and adaptive skills ($p = 0.04$). The quantity and type of enzyme proteins (no protein, single homotetramers, or multiple homo and heterotetramers), as well as their structural and functional impairments (catalytic or stability, folding, or oligomerization), contribute to phenotype severity in SSADHD. These findings are valuable for assessment of disease prognosis and management, including patient selection for gene replacement therapy. Furthermore, they provide a roadmap to determine genotype-to-protein-to-phenotype relationships in other autosomal recessive disorders.

Introduction

Succinic semialdehyde dehydrogenase deficiency (SSADHD) (OMIM #271980) is a rare [prevalent in ~ 1/460,000 (Martin et al. 2021)] inherited metabolic disorder caused by autosomal recessive inheritance of *ALDH5A1* sequence variants (Pearl et al. 2015). Enzyme deficiency results in impaired γ-aminobutyric acid (GABA) catabolism and its accumulation along with other GABA-related metabolites such as guanidinobutyrate (GBA) and γ-hydroxybutyrate (GHB). The phenotype ranges in the severity of a broad spectrum of non-pathognomonic symptoms [cognitive and adaptive deficits, Autism Spectrum Disorder, movement disorders, seizures, sleep disturbances, and psychiatric manifestations such as inattention, hyperactivity, and obsessive–compulsive behaviors (Pearl et al. 2003)]. Attempts to develop gene therapy for SSADHD are ongoing (Lee et al. 2021), but current treatment options remain supportive.

ALDH5A1 spans > 38kB on chromosome 6p22 and has an open reading frame of 1605 base pairs that encodes 535 amino acids. Its resultant protein, SSADH, is a mitochondrial enzyme composed of identical monomers arranged in a tetrameric quaternary structure. The crystal structure of human SSADH shows that each monomer comprises an NAD^+ binding domain (amino acids 1–173, 196–307, and 509–524), a catalytic domain (amino acids 308–508), and an oligomerization domain (amino acids 174–195 and 525–535) (Kim et al. 2009). Sixteen identified missense mutations determine the substitution of amino acids in different protein domains, impacting both its structure and function. For six of these missense mutations, a preliminary

Mariarita Bertoldi and Phillip L. Pearl: equal contribution.

Extended author information available on the last page of the article

prediction of their amino acid alteration consequence has been proposed based on the combination of visualization of the affected residues' position in the crystal structure (Kim et al. 2009) and data of activity cell-free extracts (Kim et al. 2009; Akaboshi et al. 2003).

A lack of a clear correlation between genotype to disease-specific phenotype (DiBacco et al. 2020) hinders our ability to define disease management criteria, offer definite prognostic counseling, and develop novel therapies for SSADHD. This study, which includes the largest cohort of genetically confirmed SSADHD subjects, aimed first to investigate how *ALDH5A1* sequence variants structurally and functionally impact the enzyme SSADH. This was accomplished by in silico mutagenesis and in-depth bioinformatic analyses of the chemical and network effects resulting from the substitution of each SSADH residue. The results of these analyses yielded subgroups of quantitative, structural, and functional SSADH molecular impairments. The study's second aim was to correlate between these subgroups to outcomes of clinical, neurophysiological, biochemical, and neuroimaging assessments representing the clinical phenotype of SSADHD.

Methods

Settings and population

This study presents an analysis of data gathered from a natural history study of SSADHD (ClinicalTrials.gov ID: NCT03758521; Boston Children's Hospital Institutional Review Board #P00029917), a prospective and multinational study commenced in 2018 by investigators of the SSADH Deficiency Research Consortium and funded by a grant to Washington State University from the National Institutes of Health (NIH R01 1R01HD091142). Clinical assessments and specimen collections were performed at three main clinical sites [Boston Children's Hospital (BCH) in the United States, University Children's Hospital Heidelberg (UCHH) in Germany, and Hospital Sant Joan Déu Barcelona Children's Hospital (UDB) in Spain] with the University of Florida providing data management. In silico mutagenesis and bioanalytical variant analyses were performed by collaborators at the University of Verona, Italy.

After being genetically confirmed with SSADHD, subjects enrolled in the natural history study undergo a series of clinical and laboratory assessments biennially. Disease severity is measured using a validated clinical severity score (CSS) obtained at bedside during study visits (Tokatly Latzer et al. 2023a). The CSS is a composite score obtained by scoring the severity of five domains representing the main manifestations of SSADHD: cognitive function, communication, motor function, psychiatric manifestations, and epilepsy. Each domain is scored on a 1–5 scale (1 indicating the most severe clinical phenotype). Participants also undergo neuropsychological evaluations, magnetic resonance imaging (MRI) and magnetic resonance spectroscopy (MRS), electroencephalography (EEG), blood collection for GABA, GHB, and γ-guanidinobutyrate (GBA), and transcranial magnetic stimulation (TMS) studies, the latter which are only completed at the BCH site.

Bioinformatics analyses assessing missense, deletion, or insertion mutations

The functionality of SSADH variants was determined using web-available bioinformatics tools based on the variants' effect on polypeptide chains (truncation or amino acid substitution). Scale-invariant feature transform (SIFT) predicted whether the variant is deleterious or tolerated, and Polymorphism Phenotyping v2 (POLYPHEN2) scored the variant as probably *or* possibly damaging. Gibbs free energy change (ΔΔG, kcal/mol) was used to assess the stability of SSADH variants (destabilizing unfavorable, destabilizing favorable, stabilizing favorable) and determined using CUPSAT (Parthiban et al. 2006). These methods refer to the single polypeptide chain and do not consider the fact that SSADH is a functional oligomer assembled by four monomeric polypeptide chains (Kim et al. 2009). This resulted in different possible SSADH polypeptide chain combinations based on the patient's genotype (Bisello and Bertoldi 2022). Homozygotic missense mutations are presumed to lead to the same amino acid alteration and synthesize the same SSADH polypeptide. Compound heterozygotes are predicted to synthesize two SSADH polypeptide chains, each with a different amino acid change. The theoretical random combination of these polypeptide chains leads to different homo and heterotetrameric species. If the genetic variant (insertion or deletion) results in a premature stop codon on both alleles, a functional SSADH protein would not be synthesized. However, in compound heterozygotes, it may lead to only one functional homotetrameric SSADH (Bisello and Bertoldi 2022). BindProfX was used to predict changes in the binding affinity of monomers to form dimers or tetramers upon variation in the form of ΔΔG values, based on an algorithm that combines FoldX physics-based potentials with conservation scores from pairs of protein–protein interaction surface sequence profiles. Conservation analyses were performed with the Consurf Server (https://consurf.tau.ac.il/) using the human SSADH amino acidic sequence as input data. A conservation score from 1 (variable residue) to 9 (conserved residue) has been attributed to each residue. Standard molecular diagnostic mutation nomenclature was followed (Ogino et al. 2007).

In silico analysis of amino acid substitutions in SSADH protein variants

Structural analysis and in silico mutagenesis of the three-dimensional structure of human SSADH (PDB: 2W8N) solved by Kim et al. (2009) was carried out by PyMOL Molecular Graphics System (version 2.5.2, Schrödinger LLC.). The types of substitution, residue localization, microenvironment, and interactions were analyzed. The lower strain value expressed by the software from the in silico mutagenesis was exploited to choose the more stable rotamer and as an informative factor for steric hindrance caused by the substitution of the wild-type amino acid residue with the amino acid substituted as a result of the patient's missense mutation. Molecular interactions between residues were identified in a surrounding area of 5 Å by means of the web tool Mol* Viewer (Sehnal et al. 2021).

Splice site analysis of intronic variants

Analysis of splice-site variants was performed using SpliceAI (2023), an interface for splicing prediction ideal for intronic variants that are ± 50 bp from exon borders. The Δ score achieved by this method for each splice-site variant ranges from 0 to 1 and can be interpreted as the probability that the variant affects splicing at any position within a window around it (± 50 bp by default) (Jaganathan et al. 2019). A Δ cut-off score > 0.5 confidently denotes aberrant splicing has occurred; scores > 0.8 indicate the prediction is highly precise; scores ranging from 0.2To 0.5 assume the occurrence of alternative splicing with production of an aberrant and normal transcript; and scores < 0.2 imply the variant had no effect.

Clinical and neurophysiological assessments

Neuropsychological assessments

Neuropsychological tests evaluated cognitive and adaptive skills [Mullen Scales of Early Learning (Mullen 1995); Differential Abilities Scale, 2nd Edition (Beran and Elliott 2007); Wechsler Abbreviated Scales of Intelligence (Wechsler 1999); Vineland Adaptive Behavior Scales, 2nd Edition (Sparrow et al. 2005)], language capacity [Receptive Language and Expressive Language, REEL-3 (Bzoch et al. 2003)], primary communication [Autism Diagnostic Observation Scale-2, ADOS-2 (Lord et al. 2012)], motor function [Movement Assessment Battery for Children- 2nd Edition (Henderson et al. 2007)], and psychiatric and behavioral attributes [Achenbach Child or Adult Behavior Checklist (CBCL or ABCL, respectively) (Achenbach and Rescorla 2000, 2001, 2003)].

Magnetic resonance imaging and spectroscopy

MRIs are done by a whole-body 3-Tesla MRI scanner (Siemens Skyra, Erlangen, Germany). Estimations of GABA/N-acetylaspartate (NAA) ratios result from two acquisitions (TR 1500 ms; TE 68 ms; bandwidth 1200 Hz) of GABA-specific MEGA-PRESS sequences of a single voxel sized $27cm^3$ (30 mm × 30 mm × 30 mm). The first acquisition includes a 1.9 ppm-arranged editing pulse allowing selective refocusing of the GABA multiplet at 3.0 ppm, and a second acquisition allocates the inversion from another location, enabling to determine GABA's J-evolution. The basal ganglia region is sampled since in SSADHD, MRI abnormalities were most consistently detected in this area (Afacan et al. 2021). The posterior cingulate and occipital cortices are sampled for their reliability to determine GABA measurements (Peek et al. 2021; Duncan et al. 2019; Costigan et al. 2019). Spectroscopy data are processed by the LCModel9 software (version 6.3) (Provencher 2021).

Electroencephalography

EEGs are done as 21-channel digital studies (Natus® NeuroWorks® EEG Software, Natus Medical Incorporated, Ontario, Canada) lasting ~ 30 min, with electrodes placed according to the 10/20 International System capture awake and sleep states. Parameters of bipolar and referential electrode montages consist of a 512 Hz sampling rate and 24-bit analog-to-digital conversion.

Transcranial magnetic stimulation

TMS is applied using the Nexstim 5.1.1 system (Nexstim, Finland). Each participant's anatomical T1-weighted MRI sequence is used for co-registration and frameless stereotaxy. The primary motor cortex is detected using a figure-of-eight coil, while motor-evoked potentials are recorded from the contralateral abductor pollicis brevis (APB) muscle (Tsuboyama et al. 2020). Electromyography (EMG) is recorded at 3 kHz using a bandpass filter ranging between 10 and 500 Hz. Resting motor threshold (rMT) is defined as the operational minimum machine output required to elicit a motor-evoked potential ≥ 50 μV from the target resting muscle in > 50% of trials. Cortical silent period (CSP) is defined as the duration from stimulation at 150% rMT to the spontaneous return of voluntary EMG-detected muscle activity on the target muscle. Long-interval cortical inhibition (LICI), defined as the log transformation of the peak-to-peak amplitude of the second pulse's resultant MEP from the peak-to-peak amplitude of the first pulse's resultant MEP, was estimated by pairs of

stimulations delivered at 120% rMT with interpulse intervals lasting 100 ms. Analysis of EMG signals was performed via LabChart v8.1.17 to extract the CSP and LICI metrics.

Plasma GABA and GABA-related gene expression

Plasma GABA, GHB, and GBA concentrations were determined after hydrolysis with 6N HCl through stable isotope dilution liquid chromatography-mass spectrometry (Arning et al. 2022). The expression of key GABA-related genes (*ALDH5A1, Abat, Glud1, GLS*) was determined in whole blood collected in PAXgene tubes. RNA extraction was performed using a PAXgene Blood miRNA Kit (QIAGEN, cat no. 763134, Hilden, Germany). RNA quality and concentration were determined using a Fragment Analyzer System Kit (cat. no. DNF-472-0500, Agilent, Santa Clara, CA) and the Qubit RNA HS assay kit (Invitrogen, cat. no. Q32855, Waltham, MA). cDNA was obtained using the RT2 First Strand Kit (QIAGEN, cat no. 330404) and loaded into a 384-well custom RT2 Profiler array (QIAGEN, Hilden, Germany). qPCR was performed using a CFX 384 (Bio-Rad Laboratories, Hercules, CA). Gene expression was normalized to *GAPDH* expression and expressed as $2^{-\Delta Ct}$.

Statistical analyses

Data were analyzed using SPSS Statistics (IBM SPSS Statistics, Version 28, 2021, IBM Corp, Armonk, NY, USA). Categorical variables are reported as their relative frequencies, whereas continuous variables are reported as either mean ± standard deviations (mean ± SD) or median and interquartile ranges (IQR) after testing for distribution normality. Group comparison and correlations were performed using either parametric tests (*t* test, one-way ANOVA, and Pearson correlation) or non-parametric tests (Mann–Whitney, Kruskal–Wallis, and Spearman's rank correlation) as appropriate. Significance level thresholds of multiple comparisons were corrected by the Bonferroni-Dunn method. Relationships between genotypes and phenotypic variables known to be age-dependent (e.g., plasma GABA, GHB, and GBA, MRS-derived GABA/NAA ratio, and TMS-derived rMT and CSP) were analyzed using a linear regression model that included age as a covariate to obtain estimates of the differences between subgroups' marginal means and their standard errors. A p value ≤ 0.05 was considered significant for all analyses.

Results

The study included the genetic information of 58 (1:1 male/female ratio) individuals from 50 unrelated families with 32 *ALDH5A1* allelic variants, eight of which were previously unreported (c.104_127 del, c.127delC, c.870 + 1G>T, 6p22.3 deletion, c.644_647delTGGG, c.1558G>C, c.755G>A, and c.1388del) (Table 1). The most common sequence variants were c.1226G>A (16%), c.612G>A (16%), and c.803G>A (9%) (Fig. 1). Of the 116 affected alleles, 64 variants (55%) were missense, 23 non-sense (20%), 16 splice-site (14%), and 12 frameshift (10%) (10 deletions and 2 duplications). An additional variant included the deletion of chromosome 6p22.3 in its entirety. Twenty-three subjects (40%) were homozygotes, and 35 (60%) compound heterozygotes for these variants, resulting in either a truncated/no protein [N = 16 (28%)], a single homotetrameric protein with [N = 35 (60%)], or a mixed population of homo and heterotetrameric proteins [N = 7 (12%)]. A functional analysis based on the domain where the amino acid subjected to substitution is located and on the impact of the substitution on the binding strength of the affected intramolecular network determined that SSADH proteins were either impaired in stability, folding, and oligomerization [N = 29 (50%)] or in catalytic activity [N = 13 (22%)] (Table 2).

In silico analyses

According to the computational predictive tools POLYPHEN-2, SIFT, and CUPSTAT, all missense variants were determined to have a pathogenic clinical significance (Table 1) in accordance with the American College of Medical Genetics and Genomics (ACMG) standards and guidelines (Richards et al. 2015). The variants' functional consequences were investigated by studying the crystal structure of the SSADH enzyme. Initially, variants were mapped to the known domains of the protein: C93F, A139D, R173C, G196D, P203L, G252C, G252D, G252V, G268E, and G520R were mapped to the NAD^+ binding domain; N335K, G409D, M432L, and G441R to the catalytic domain; and G176R and G533R to the oligomerization domain (Table 1, Fig. 2). Variants mapping to the NAD^+ binding domain all lead to varying degrees of destabilizing or misfolding of the alpha/beta structure essential to the integrity of the NAD^+ binding site. Since this domain is large, the functional effects of variants could vary depending on whether they lie on the surface of the NAD^+ binding site, the NAD^+ binding groove, or in the secondary structures surrounding the site. This possibility led us to perform additional analyses of the spatial structure of each affected residue and refine our prediction of the effects of variants on protein function. C93 is present in a hydrophilic cluster (Fig. 2A), and the C93F substitution (c.278G>T) changes its interactions with nearby residues, leading to the collision of a bulky aromatic side chain with several structural elements and disruption of this domain's stability. A139 lies within a hydrophobic interface between two antiparallel alpha-helices of the same monomer, with carbonyl and amidic moieties providing stabilizing polar

Table 1 *In-Silico* analyses of the 32 *ALDH5A1* allelic variants found in SSADHD individuals of this study

Nucleotide Variant	Protein Variant	Exon/Intron	Domain	SpliceAI Δscore (Hogema et al. 2001)	CONSURF	BINDPROFX ΔΔG (Kcal/mol)	SIFT	POLY-PHEN-2	CUPSAT Atom potential Torsion potential Mean ΔΔG (Kcal/mol)	Known or Predicted Molecular Effect (Crystal Structure Inspection)	References
c.612G>A	W204X	Exon 4	NAD^+ binding							Production of a truncated and inactive subunit	Hogema et al. (2001)
c.1234C>T	R412X	Exon 8	Catalytic domain							Production of a truncated and inactive subunit	Hogema et al. (2001)
c.1015-2A>C	Splice site	Intron 7		0.99 (loss) 0.88 (gain)						Production of a truncated and inactive subunit	Akaboshi et al. (2003)
c.1597G>A	G533R	Exon 10	Oligomerization		6	0.511	0.01 deleterious	1.0 Probably damaging	Destabilizing Unfavorable − 1.27	Possible misfolding and/or oligomerization impairment (Kim et al. 2009)	Akaboshi et al. (2003)
c.608C>T	P203L	Exon 3	NAD^+ binding		8		0.00 deleterious	1.0 Probably damaging	Destabilizing Unfavorable − 3.85	Possible interference with NAD^+ binding (diphosphate moiety of ADP) and catalytic impairment	Attri et al. (2017)
c.803G>A	G268E	Exon 5	NAD^+ binding		7		0.00 deleterious	1.0 Probably damaging	Stabilizing Favorable 1.95	Possible interference with NAD^+ binding (ADP moiety) and catalytic impairment (Kim et al. 2009)	Chambliss et al. (1995)

Table 1 (continued)

Nucleotide Variant	Protein Variant	Exon/Intron	Domain	SpliceAI Δscore (Hogema et al. 2001)	CONSURF	BINDPROFX ΔΔG (Kcal/mol)	SIFT	POLYPHEN-2	CUPSAT Atom potential Torsion potential Mean ΔΔG (Kcal/mol)	Known or Predicted Molecular Effect (Crystal Structure Inspection)	References
c.967_968dupCA	Q323HfsX3	Exon 6	Catalytic domain							Production of a truncated and inactive subunit	DiBacco et al. (2020)
c.1226G>A	G409D	Exon 8	Catalytic domain		5		0.00 deleterious	1.0 Probably damaging	Destabilizing Favorable − 0.1	Steric hindrance and expected misfolding/destabilization effects (Kim et al. 2009)	Hogema et al. (2001)
c.1323dupG	P442AfsX18	Exon 8	Catalytic domain							Production of a truncated and inactive subunit	Akaboshi et al. (2003)
c.870 + 3delA	Splice site	Intron 5		0.75 (loss)						Production of a truncated and inactive subunit	DiBacco et al. (2020)
c.526G>A	G176R	Exon 3	Oligomerization		2	0.000	0.00 deleterious	1.0 Probably damaging	Destabilizing Unfavorable − 0.85	Possible misfolding and/or oligomerization impairment (Kim et al. 2009)	Akaboshi et al. (2003)
c.416C>A	A139D	Exon 2	NAD^+ binding		7		0.01 deleterious	1.0 Probably damaging	Destabilizing Unfavorable − 0.97	Destabilizing effect for insertion of a polar residue into a hydrophobic cluster	DiBacco et al. (2020)
c.104_127 del	S35X	Exon 1	Mitochondrial targeting sequence							Production of a truncated and inactive subunit	

Table 1 (continued)

Nucleotide Variant	Protein Variant	Exon/Intron	Domain	SpliceAI Δscore (Hogema et al. 2001)	CONSURF	BINDPROFX ΔΔG (Kcal/mol)	SIFT	POLYPHEN-2	CUPSAT Atom potential Torsion potential Mean ΔΔG (Kcal/mol)	Known or Predicted Molecular Effect (Crystal Structure Inspection)	References
c.517C>T	R173C	Exon 3	NAD^+ binding		2		0.00 deleterious	1.0 Probably damaging	Stabilizing Favorable 0.58	Possible oligomerization impairment due to alteration in polarity	Pearl et al. (2015)
c.1321G>A	G441R	Exon 8	Catalytic domain		8		0.00 deleterious	1.0 Probably damaging	Destabilizing Unfavorable − 3.15	Destabilization due to insertion of a bulky polar residue	DiBacco et al. (2020)
c.1402+2T>C	Splice site	Intron 9		0.97 (loss)						Production of a truncated and inactive subunit	DiBacco et al. (2020)
c.278G>T	C93F	Exon 1	NAD^+ binding		7		0.63 tolerated	0.999 Probably damaging	Stabilizing Unfavorable 2.16	Insertion of an apolar/bulky residue in a buried cleft; possible misfolding defect/destabilization (Kim et al. 2009)	Akaboshi et al. (2003)
c.1015-3C>G	Splice site	Intron 7		0.39 (loss) 0.40 (gain)						Production of a truncated and inactive subunit	DiBacco et al. (2020)

Table 1 (continued)

Nucleotide Variant	Protein Variant	Exon/Intron	Domain	SpliceAI Δscore (Hogema et al. 2001)	CONSURF	BINDPROFX ΔΔG (Kcal/mol)	SIFT	POLYPHEN-2	CUPSAT Atom potential Torsion potential Mean ΔΔG (Kcal/mol)	Known or Predicted Molecular Effect (Crystal Structure Inspection)	References
c.754G>T	G252C	Exon 5	NAD^+ binding		4		0.00 deleterious	1.0 Probably damaging	Destabilizing Unfavorable − 8.12	Expected alteration of the local hydrophobicity possibly leading to a misfolding defect	Pop et al. (2020)
c.621delC	S208VfsX3	Exon 4	NAD^+ binding							Production of a truncated and inactive subunit	Akaboshi et al. (2003)
c.127delC	Q43SfsX47	Exon 1	Mitochondrial targeting sequence							Production of a truncated and inactive subunit	
c.587G>A	G196D	Exon 3	NAD^+ binding		9		0.00 deleterious	1.0 Probably damaging	Destabilizing Unfavorable − 8.19	Expected alteration of the secondary and tertiary structure; possible misfolding defects	Jansen et al. 2008)
c.870 + 1G>T	Splice site	Intron 6		0.75 (loss)						Production of a truncated and inactive subunit	
Deletion 6p22.3	No SSADH synthesis									No SSADH protein	
c.644_647delTGGG	V215GfsX11	Exon 4	NAD^+ binding							Production of a truncated and inactive subunit	

Table 1 (continued)

Nucleotide Variant	Protein Variant	Exon/Intron	Domain	SpliceAI Δscore (Hogema et al. 2001)	CONSURF	BINDPROFX ΔΔG (Kcal/mol)	SIFT	POLYPHEN-2	CUPSAT Atom potential Torsion potential Mean ΔΔG (Kcal/mol)	Known or Predicted Molecular Effect (Crystal Structure Inspection)	References
c.1558G>C	G520R	Exon 10	NAD^+ binding		6		0.01 deleterious	1.0 Probably damaging	Destabilizing Favorable − 2.17	Possible misfolding and/or oligomerization impairment (Kim et al. 2009)	
c.755G>T	G252V	Exon 5			4		0.00 deleterious	1.0 Probably damaging	Destabilizing Unfavorable − 7.04	Possible misfolding defects	Pop et al. (2020)
c.755G>A	G252D	Exon 5			4		0.13 tolerated	1.0 Probably damaging	Destabilizing Unfavorable − 4.48	Possible folding defects	
c.1294A>C	M432L	Exon 8	Catalytic domain		5		0.09 tolerated	0.700 Possibly damaging	Destabilizing Unfavorable − 0.67	Possible defects in folding and/or catalysis	Yamakawa et al. (2012)
c.610-2A>G	Splice site	Intron 4		0.96 (loss) 0.44 (gain)						Production of a truncated and inactive subunit	Akaboshi et al. (2003)
c.1005C>A	N335K	Exon 6	Catalytic domain		8		0.05 deleterious	0.999 Probably damaging	Destabilizing Unfavorable − 1.01	Expected alteration of the local charge, possible influence on catalysis	Akaboshi et al. (2003)
c.1388del	D463VfsX2	Exon 9	Catalytic domain		8					Production of a truncated and inactive subunit	

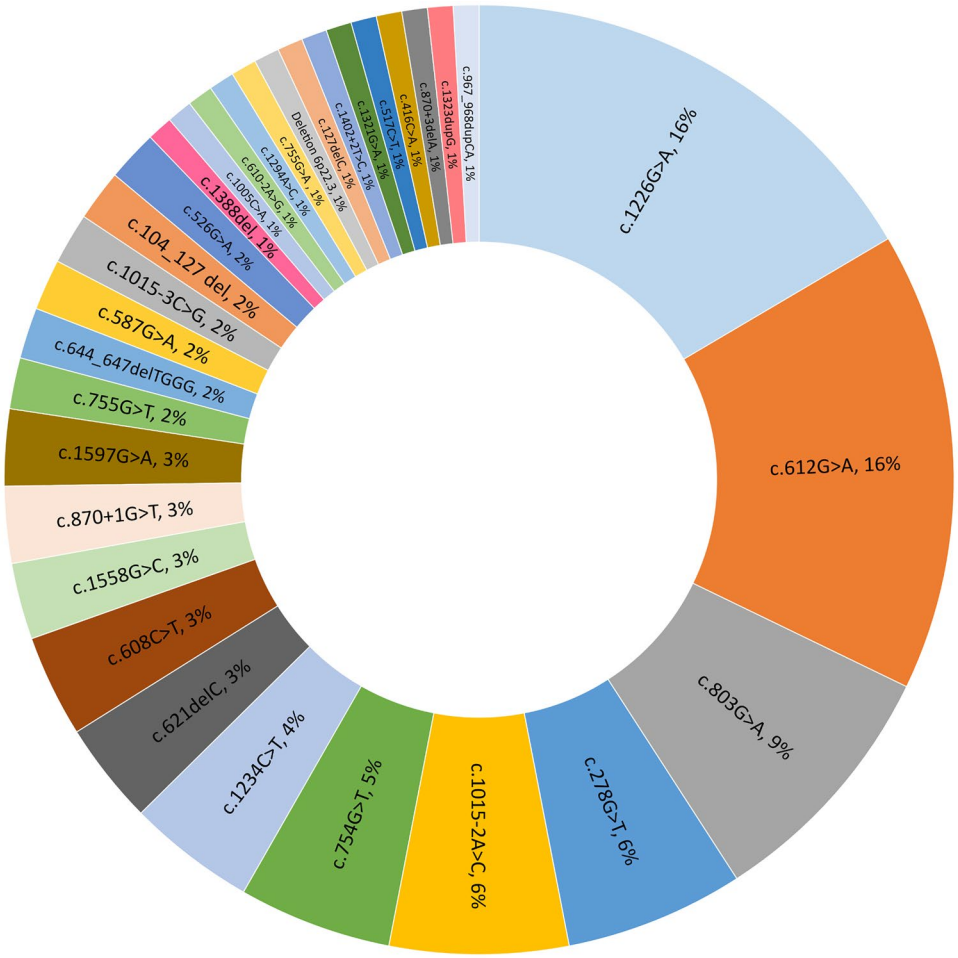

Fig. 1 Rate of occurrence of 32 ALDH5A1 variants in 58 individuals with succinic semialdehyde dehydrogenase deficiency

interactions. The A139D substitution (c.416C>A) destroys the hydrophobic interface, leading to the disassembly of the alpha helices and domain destabilization (Fig. 2B). A173 is positioned at the edge of the NAD^+ domain and is critical to maintaining the quaternary SSADH tetrameric structure assembled as a dimer of dimers (Kim et al. 2009). A173 of one monomer faces the opposite monomer leading to the dimeric structure that will interact with an identical dimer to form the tetramer. The A173C substitution (c.517C>T) leads to the loss of interchain integrity while intrachain bonds remain stabilized by other means (Fig. 2C). G196 is involved in the linkage of two β sheets and is vital for stabilizing the entire NAD^+ binding domain. The G196D substitution (c.587G>A) alters the stacking interactions of the two β-sheets (Fig. 2D) and destabilizes the NAD^+ binding domain. P203, located in a buried residue within a hydrophobic cluster that accommodates the phosphate moiety of the coenzyme's ADP portion, correctly positions the catalytic loop (residues 334–344). The P203L substitution (c.608C>T) alters the conformational rigidity of the residue and weakens the network bond (Fig. 2E). G252 resides in a loop connecting secondary structure elements responsible for the large eight stacked β-sheets composing the NAD^+ domain, which is stabilized by an extensive H-bond network. When substitutions such as G252V (c.755G>T) (predicted to be the worst), G252C (c.754G>T), or G252D (c.755G>A) occur, polar and sterically bulkier residues are introduced into the hydrophobic moiety of the beta sheets and the fold of the eight-β-sheets element is compromised (Fig. 2F). G268 has a fundamental role in maintaining the stability of an α-helix essential for NAD^+ binding. The G268E substitution (c.803G>A) loosens the structurally essential interactions of this region (Fig. 2G). Finally, G520 takes part in maintaining the secondary structure motif preceding the C-terminal by reinforcing an H-bond-backbone with other residues. Accordingly, the G520A substitution (c.1558G>C) leads to the disassembly of this region and deleterious protein misfolding (Fig. 2H).

The effects played by variants mapping at the catalytic domain are severe. N335K, by directly altering the catalytic loop, leads to larger functional than structural impairment. Alternatively, G409D, M432L, and G441R destabilize the architecture of the catalytic domain, resulting in its structural disassembly. In more depth, N335 belongs to

Table 2 Allelic variants, zygosity, resultant proteins combination, and eventual protein impairment effect of the SSADHD patients included in the study

Patient	Allele_1	Allele_2	Zygosity	Protein variants combination	Effect
1	c.612G>A	c.612G>A	Homozygosis	Truncated protein	No protein
2	c.612G>A	c.1234C>T	Compound heterozygosis	Truncated proteins	No protein
3	c.612G>A	c.1234C>T	Compound heterozygosis	Truncated proteins	No protein
4	c.612G>A	c.1015-2A>C	Compound heterozygosis	Truncated protein/impaired splicing	No protein
5	c.1015-2A>C	c.1597G>A	Compound heterozygosis	Hemizygote G533R homotetramers	Oligomerization
6	c.608C>T	c.608C>T	Homozygosis	P203L homotetramer	Catalysis
7	c.612G>A	c.803G>A	Compound heterozygosis	Hemizygote G268E homotetramers	Catalysis
8	c.967_968dupCA	c.1597G>A	Compound heterozygosis	Hemizygote G533R homotetramers	Oligomerization
9	c.1226G>A	c.1323dupG	Compound heterozygosis	Hemizygote G409D homotetramers	Stability/folding
10	c.612G>A	c.870 + 3delA	Compound heterozygosis	Truncated protein/impaired splicing	No protein
11	c.526G>A	c.1226G>A	Compound heterozygosis	Mixed protein population of G409D and G176E homotetramers and heterotetramers	Folding/stability and oligomerization
12	c.1015-2A>C	c.416C>A	Compound heterozygosis	Hemizygote A139D homotetramers	Stability/folding
13	c.517C>T	c.1015-2A>C	Compound heterozygosis	Hemizygote R173C homotetramers	Oligomerization
14	c.104_127 del	c.1015-2A>C	Compound heterozygosis	Truncated protein/impaired splicing	No protein
15	c.104_127 del	c.1015-2A>C	Compound heterozygosis	Truncated protein/impaired splicing	No protein
16	c.612G>A	c.1321G>A	Compound heterozygosis	Hemizygote G441R homotetramers	Stability/folding
17	c.612G>A	c.1402 + 2T>C	Compound heterozygosis	Truncated protein/impaired splicing	No protein
18	c.612G>A	c.803G>A	Compound heterozygosis	Hemizygote G268E homotetramers	Catalysis
19	c.278G>T	c.1015-3C>G	Compound heterozygosis	Hemizygote C93F homotetramers	Stability/folding
20	c.612G>A	c.803G>A	Compound heterozygosis	Hemizygote G268E homotetramers	Catalysis
21	c.1226G>A	c.1226G>A	Homozygosis[a]	G409D homotetramers	Stability/folding
22	c.754G>T	c.754G>T	Homozygosis[a]	G252C homotetramers	Stability/folding
23	c.754G>T	c.754G>T	Homozygosis[a]	G252C homotetramers	Stability/folding
24	c.754G>T	c.754G>T	Homozygosis[a]	G252C homotetramers	Stability/folding
25	c.1226G>A	c.1226G>A	Homozygosis[a]	G409D homotetramers	Stability/folding
26	c.612G>A	c.1597G>A	Compound heterozygosis	Hemizygote G533R homotetramers	Oligomerization
27	c.612G>A	c.803G>A	Compound heterozygosis	Hemizygote G268E homotetramers	Catalysis
28	c.612G>A	c.803G>A	Compound heterozygosis	Hemizygote G268E homotetramers	Catalysis
29	c.621delC	c.621delC	Homozygosis[a]	Truncated/inactive	No protein
30	c.127delC	c.803G>A	Compound heterozygosis	Hemizygote G268E homotetramers	Catalysis
31	c.1234C>T	c.1234C>T	Homozygosis	Truncated/inactive	No protein
32	c.870 + 1G>T	c.870 + 1G>T	Homozygosis[a]	Truncated/inactive	No protein

Table 2 (continued)

Patient	Allele_1	Allele_2	Zygosity	Protein variants combination	Effect
33	c.870 + 1G>T	c.870 + 1G>T	Homozygosis[a]	Truncated/inactive	No protein
34	c.278G>T	c.621delC	Compound heterozygosis	Hemizygote C93F homotetramers	Stability/folding
35	c.278G>T	c.621delC	Compound heterozygosis	Hemizygote C93F homotetramers	Stability/folding
36	c.526G>A	Deletion 6p22.3	Compound heterozygosis	Hemizygote G176E homotetramers	Folding/oligomerization
37	c.278C>T	c.803G>A	Compound heterozygosis	Mixed protein population of C93F and G268E homotetramers and heterotetramers	Catalysis[b]
38	c.278G>T	c.278G>T	Homozygosis	C93F homotetramers	Stability/folding
39	c.587G>A	c.587G>A	Homozygosis	G196D homotetramers	Stability/folding
40	c.644_647delTGGG	c.644_647delTGGG	Homozygosis	Truncated/inactive	No protein
41	c.1226G>A	c.1558G>C	Compound heterozygosis	Mixed protein population of G409D and G520R homotetramers and heterotetramers	Stability/folding and oligomerization
42	c.612G>A	c.612G>A	Homozygosis	Truncated protein	No protein
43	c.612G>A	c.612G>A	Homozygosis	Truncated protein	No protein
44	c608C>T	c608C>T	Homozygosis	P203L homotetramer	Catalysis
45	c.1226G>A	c.1226G>A	Homozygosis[a]	G409D homotetramers	Stability/folding
46	c.755G>T	c.755G>T	Homozygosis	G252V homotetramers	Stability/folding
47	c.755G>A	c.1226G>A	Compound heterozygosis	Mixed protein population of G252D and G409D homotetramers and heterotetramers	Stability/folding
48	c.610-2A>G	c.1294A>C	Compound heterozygosis	Hemizygote M432L homotetramers	Catalysis
49	c.1005C>A	c.1015-2A>C	Compound heterozygosis	Hemizygote N335K homotetramers	Catalysis
50	c.1226G>A	c.278G>T	Compound heterozygosis	Mixed protein population of C93F and G409D homotetramers and heterotetramers	Stability/folding
51	c.1226G>A	c.1226G>A	Homozygosis	G409D homotetramers	Stability/folding
52	c.1226G>A	c.1226G>A	Homozygosis	G409D homotetramers	Stability/folding
53	c.1226G>A	c.1226G>A	Homozygosis	G409D homotetramers	Stability/folding
54	c.1226G>A	c.1226G>A	Homozygosis	G409D homotetramers	Stability/folding
55	c.1234C>T	c.1015-3C>G	Compound heterozygosis	Truncated protein/impaired splicing	No protein
56	c.803G>A	c.1558G>C	Compound heterozygosis	Mixed protein population of G268E and G520R homotetramers and heterotetramers	Catalysis[b]
57	c.803G>A	c.1558G>C	Compound heterozygosis	Mixed protein population of G268E and G520R homotetramers and heterotetramers	Catalysis[b]
58	c.1388del	c.803G>A	Compound heterozygosis	Hemizygote G268E homotetramers	Catalysis

[a]Consanguinity

[b]Also a minor effect in stability/folding

the catalytic loop (Kim et al. 2009) and maintains its orientation by means of an H-bond network. With the N335K substitution (c.1005C>A), the binding of succinic semialdehyde to its pocket is hindered (Fig. 2I). Since aspartate is a polar residue, the G409D substitution (c.1226G>A) destabilizes the superficial part of the β-sheet to which it belongs (Fig. 2J). The M432L replacement (c.1294A>C) alters the steric hindrance of this residue, possibly leading to erroneous rearrangement of nearby structures (Fig. 2K). Lastly, G441 belongs to a loop connecting structural

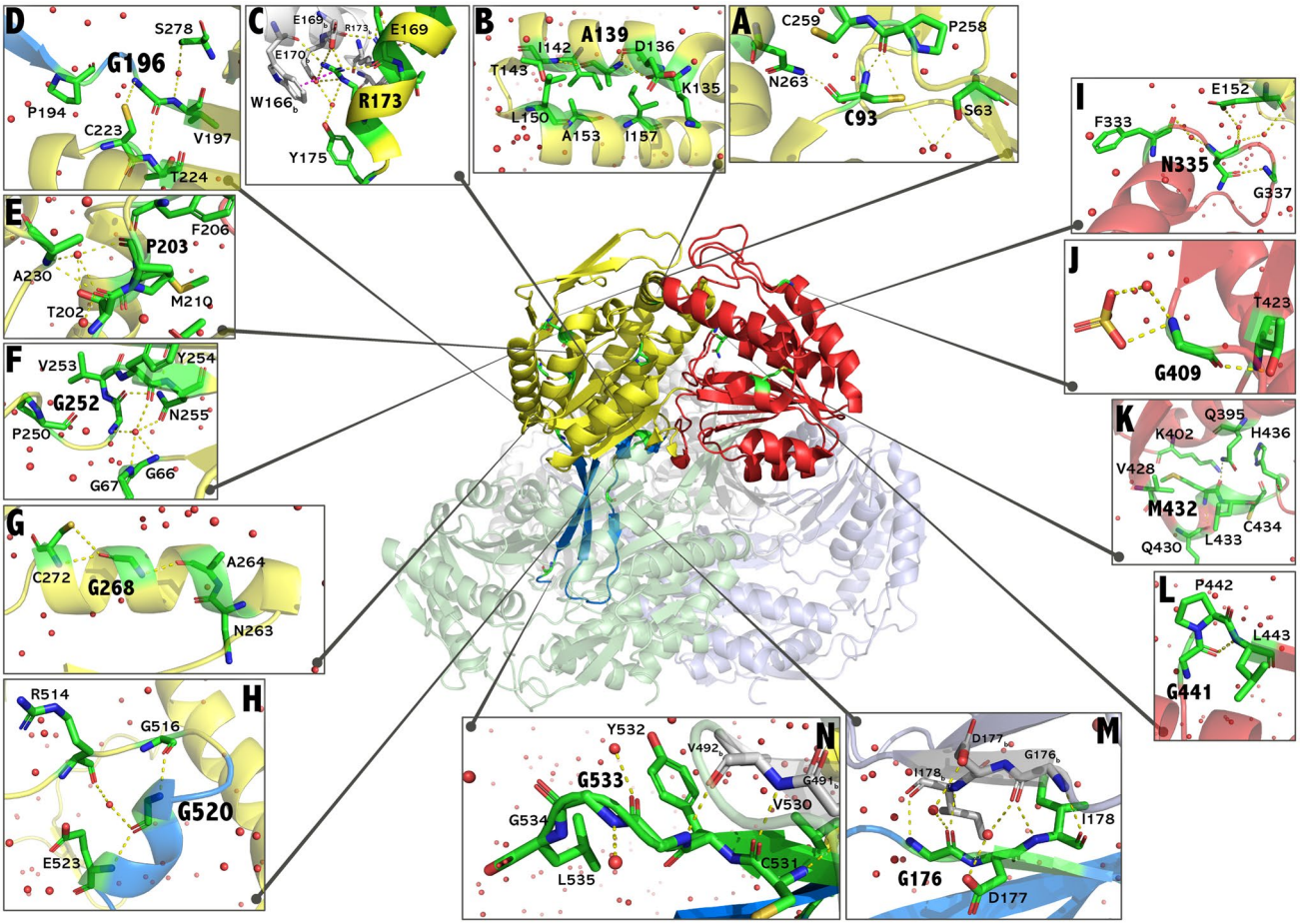

Fig. 2 Representation of the SSADH amino acids subjected to substitution. Ribbon representation of the tetrameric assembly of human SSADH (PDB: 2W8N9) in which one monomer is colored by domain organization: NAD^+ binding domain in yellow, catalytic domain in red, and oligomerization domain in blue. The other monomers are colored white, light green, and light purple. The amino acids that are subjected to substitution are represented by green sticks. **A**–**H** Residues belonging to the NAD^+ binding domain, **I**–**L** residues belonging to the catalytic domain, and **M**, **N** residues belonging to the oligomerization domain. For each residue, the main contacts with neighboring residues are displayed. The figure is rendered with PyMol [Molecular Graphics System (version 2.5.2), Schrödinger LLC]

elements of the catalytic domain, which is destabilized by the G441R substitution (c.1321G>A) (Fig. 2L).

Variants disturbing the oligomerization domain constitute two different Glycine-to-Arginine substitutions that preserve hydrophilicity but make interactions with the other monomer onerous despite mapping distantly on the protein surface. G176 maintains the H-bonds of nearby residues, and its substitution to arginine (c.526G>A) damages the multimeric assembly of the protein (Fig. 2M). The same holds for G533 residing on SSADH's terminal loop, as its substitution by arginine (c.1597G>A) inhibits the proper stacking and inter-monomer interactions of this region (Fig. 2N).

Notably, 10/16 (62%) of the variants involve the substitution of a small glycine residue with a bulkier positively or negatively charged amino acid, resulting, at first glance, in a profound conformational effect, considering the conformational role played by glycine residues due to their relatively high degrees of freedom.

The steric hindrance resultant from neighboring residues within the monomeric structure of SSADH was highest in the variants G252V (67.95), G252C (56.81), G409D (56.27), G441R (55.84), and G252D (55.70) (Table 3), indicating a larger variation of their resultant protein from the wild-type protein. Interestingly, N335K and G176R variants have lower values of steric hindrance (Table 3) since the former affects the catalytic loop but does not play a steric effect, while the latter affects oligomerization with a neighboring monomer that is not reported by the steric hindrance calculation which is based on steric effects played on the same monomer.

Table 3 In silico evaluation of SSADHD-related variants' steric hindrance resultant from substituted neighboring residues within the monomeric structure of SSADH

Variant	Steric Hindrance
G252V	67.95
G252C	56.81
G409D	56.27
G441R	55.84
G252D	55.70
C93F	41.87
P203L	41.12
G520R	38.18
G196D	33.42
G533R	31.74
G268E	29.06
R173C	25.53
A139D	21.94
M432L	15.31
N335K	14.55
G176R	11.03

Splice-site variants analysis

Splice-site variant analysis with SpliceAI revealed that 5 out 6 of the splice-site variants (c.1015-2A>C, c.870 + 3delA, c.1402 + 2T>C, c.870 + 1G>T, c.610-2A>G) had high Δ scores (mean ± SD of 0.88 ± 0.12), indicating a high probability for aberrant splicing, alteration in the frame of the translated protein's frame, and a predicted complete lack of SSADH protein. One splicing variant (c.1015-3C>G) resulted in a lower Δ score (0.39).

Genotype-to-protein-to-phenotype correlations

Of the 58 study participants, 27 were assessed at BCH, 11 at UCHH, 10 at UDB, and 10 were from the SOC cohort. The study group had an even distribution of sexes, and participants' overall median (IQR) age at their first study visit was 9.8 (5.4–15.3) years. The ethnic distribution was 40 (69%) Caucasians, 6 (10%) Arab, 3 (5%) Asian, and 9 (15%) other ethnicities. No participant was born prematurely or had any perinatal complications. Movement disorders were present in 32 (55%) subjects: 30 (52%) had ataxia, 14 (24%) had dyskinesia, and 9 (15%) had dystonia. Thirty subjects (52%) had seizures, which were considered drug-resistant seizures (Kwan et al. 2010) in 9 (15%), and 47 (81%) had EEG abnormalities [27 (47%) with diffuse background slowing and 18 (31%) showing epileptiform activity]. The mean ± SD FSIQ was 51.0 ± 12.8 (assessed in 27 subjects), the total composite adaptive score was 60.5 ± 14.1 (assessed in 33 subjects), and 17/30 (57%) who were assessed with the ADOS-2 were diagnosed with ASD. The study group's mean ± SD total CSS was 17.2 ± 2.8.

Compared to individuals with single homotetrameric or multiple homo and heterotetrameric proteins, those with no protein had significantly lower plasma expression of *ALDH5A1* (p = 0.001). They also had lower values of the total CSS ($p = 0.008$) and lower cognitive ($p = 0.01$), epilepsy ($p = 0.04$), and psychiatric ($p = 0.04$) severity scores. Dyskinesia ($p = 0.05$), seizures ($p = 0.01$), and EEG abnormalities ($p < 0.001$) were significantly more prevalent in individuals with no protein or single homotetramers compared to those with a mixed population of homo and heterotetrameric proteins. There was no significant relationship between the number of proteins and age, sex, communication and motor CSS domain scores, FSIQ, adaptive function, Autism Spectrum Disorder, and age-adjusted cerebral GABA/NAA ratio, plasma GABA, GHB, and GBA, and TMS-derived parameters (Table 4).

An additional comparison was made between the same group of individuals with no production of SSADH protein to two other groups: the first including subjects in whom protein variants led to stability, folding, or oligomerization defects, and a second in which the resultant defect was catalytic because of affecting structural elements essential to catalysis or belonging to the NAD^+ "sitting" groove. This comparison showed that with respect to individuals with a stability, folding, or oligomerization defect, those with no protein and a catalysis/NAD + binding defect had significantly lower total scores of their total CSS ($p = 0.02$) and CSS cognitive domain ($p = 0.008$), lower adaptive function test scores ($p = 0.04$) and more subjects with dyskinesia ($p = 0.03$). There was no difference between these groups in any other phenotype parameter assessed (Table 4).

Division of the total CSSs of our study group to quartiles showed that 13 subjects were found in the top quartile (CSS ≥ 19.25), indicating the mildest clinical severity (patients #1, #5, #11, #12, #16, #23, #35, #36, #37, #47, #51, #53, #54). The vast majority (92%) of subjects from this subgroup had single homotetrameric or multiple homo or heterotetrameric SSADH proteins, *all* (100%) of which were affected by impaired stability, folding, or oligomerization. One subject (#1) from this subgroup had a combination of two nonsense variants presumed to synthesize only truncated SSADH polypeptide chains which cannot assemble the oligomeric SSADH, resulting in no functional SSADH protein produced. Out of the 18 missense variants of this subgroup, 6 (33%) were c.1226 G>A p.G409D, and 3 (17%) were c.278G>T, p.C93F (Fig. 3). Conversely, out of the 12 most severely affected subjects (#4, #14, #15, #18, #28, #29, #33, #34, #43, #44, #50, and #56) (all with CSS < 15, in the lower quartile), eight were predicted to have no protein being produced (by a combination of nonsense and splice-site variants), and four had single homotetrameric proteins, *all* (100%) which were impaired in catalysis abilities (three had one missense variant affecting catalysis that accompanied a

Table 4 Relationship between genotype expressed in clusters of protein quantity and impairment effect to clinical phenotype

Phenotype features	No protein*, N = 16 (28)	Quantitative protein groups, N = 58 (%)			Impairment effect groups, N = 58 (%)		
		Single homotetramers, N = 35 (60)	Multiple homo and heterotetramers, N = 7 (12)	*p***	Folding/stability/oligomerization, N = 29 (50)	Catalysis, N = 13 (22)	*P****
Age, years, median (IQR)	9.8 (6.9–21.5)	10.4 (5.3–15.0)	7.8 (4.2–11.1)	0.22	9.6 (4.2–14.2)	11.1 (8.0–14.4)	0.33
Sex							
Male/female	9 (56)/7 (44)	16 (46)/19 (54)	4 (57)/3 (43)	0.72	4 (31)/9 (69)	16 (55)/13 (45)	0.28
Consanguinity	3 (19)	6 (17)	0 (0)	0.45	6 (21)	0 (0)	0.19
Gene expression, 2^ΔCT							
ALDH5A1 (N = 23)	0.01 ± 0.005 (N = 8)	0.02 ± 0.01 (N = 14)	0.05 ± 0.0 (N = 1)	**0.001**	0.02 ± 0.01 (N = 11)	0.01 ± 0.008 (N = 4)	0.07
Abat (N = 23)	0.03 ± 0.03 (N = 8)	0.02 ± 0.007 (N = 14)	0.02 ± 0.0 (N = 1)	0.43	0.02 ± 0.007 (N = 11)	0.02 ± 0.009 (N = 4)	0.43
GLS (N = 23)	0.11 ± 0.04 (N = 8)	0.09 ± 0.02 (N = 14)	0.11 ± 0.0 (N = 1)	0.46	0.09 ± 0.09 (N = 11)	0.09 ± 0.004 (N = 4)	0.51
Clinical Severity Score (CSS)							
Total score	15.5 ± 2.9	17.8 ± 2.6	18.5 ± 1.3	**0.008**	18.7 ± 1.9	16.2 ± 2.6	**0.02**
Cognitive	1.9 ± 0.8	2.6 ± 0.9	2.8 ± 0.3	**0.01**	2.8 ± 0.9	2.4 ± 0.7	**0.008**
Communication	2.5 ± 0.6	2.8 ± 0.9	3.1 ± 0.9	0.27	2.9 ± 0.9	3.0 ± 1.0	0.33
Motor	3.7 ± 1.0	3.7 ± 0.8	3.2 ± 0.7	0.47	3.7 ± 0.7	3.3 ± 0.9	0.42
Psychiatry	2.6 ± 1.3	3.4 ± 1.1	4.0 ± 0.8	**0.04**	3.6 ± 1.1	3.2 ± 1.0	0.10
Epilepsy	3.6 ± 1.2	4.1 ± 1.2	5.0 ± 0.0	**0.04**	4.5 ± 1.0	3.7 ± 1.2	0.10
Neuropsychologic assessments							
FSIQ (N = 27)	47.8 ± 13.1 (N = 8)	52.1 ± 13.1 (N = 18)	57.0 ± 0.0 (N = 3)	0.67	53.3 ± 13.4 (N = 14)	49.6 ± 11.6 (N = 5)	0.62
Adaptive composite score (N = 33)	56.5 ± 11.2 (N = 9)	61.4 ± 15.1 (N = 23)	75.0 ± 0.0 (N = 3)	0.41	66.6 ± 12.9 (N = 16)	52.8 ± 15.7 (N = 8)	**0.04**
ASD assessed by ADOS-2 (N = 30)	6 (67) (N = 9)	11 (52) (N = 21)	–	0.37	6 (43) (N = 14)	5 (71) (N = 7)	0.35
Movement disorders							
Ataxia	11 (69)	17 (49)	2 (29)	0.17	8 (61)	11 (38)	0.10
Dyskinesia	7 (44)	7 (20)	0 (0)	**0.05**	3 (10)	4 (31)	**0.03**
Dystonia	2 (12)	5 (14)	2 (29)	0.58	3 (10)	4 (31)	0.22
Epilepsy							
Seizures	9 (56)	21 (60)	0 (0)	**0.01**	13 (45)	8 (61)	0.55
Drug-resistant seizures	3 (43)	6 (29)	–	0.48	2 (15)	4(50)	0.20
EEG abnormalities	15 (94)	30 (86)	2 (29)	**< 0.001**	21 (72)	11 (85)	0.31
EEG-diffuse background slowing	9 (56)	17 (49)	1 (14)	0.16	13 (45)	4 (31)	0.39
EEG-epileptiform activity	5 (31)	12 (34)	1 (14)	0.58	6 (20)	7 (54)	0.10
MRS GABA/NAA, EMM (SE)							

Table 4 (continued)

Phenotype features	No protein*, N = 16 (28)	Quantitative protein groups, N = 58 (%)			Impairment effect groups, N = 58 (%)		
		Single homotetramers, N = 35 (60)	Multiple homo and heterotetramers, N = 7 (12)	*p***	Folding/stability/oligomerization, N = 29 (50)	Catalysis, N = 13 (22)	*P****
Basal ganglia (N = 13)	0.19 (0.02) (N = 3)	0.20 (0.01) (N = 9)	–	0.56	0.19 (0.01) (N = 7)	0.22 (0.02) (N = 2)	0.62
Posterior cingulate gyrus (N = 19)	0.21 (0.01) (N = 7)	0.22 (0.01) (N = 11)	–	0.46	0.21 (0.01) (N = 8)	0.23 (0.01) (N = 3)	0.42
Occipital cortex (N = 12)	0.16 (0.01) (N = 7)	0.17 (0.02) (N = 5)	–	0.62	0.16 (0.02) (N = 3)	0.19 (0.03) (N = 2)	0.74
Biochemical metrics, EMM (SE)							
GABA, μM/L (N = 43)	3.1 (0.2) (N = 16)	2.8 (0.2) (N = 24)	3.0 (0.6) (N = 3)	0.70	2.9 (0.2) (N = 20)	2.5 (0.4) (N = 7)	0.52
GHB, μM/L (N = 34)	274.2 (224.4) (N = 11)	467.5 (154.5) (N = 22)	1009.6 (732.9) (N = 1)	0.59	580.2 (178.1) (N = 16)	243.1 (290.9) (N = 7)	0.47
GBA, μM/L (N = 29)	0.09 (0.009) (N = 9)	0.07 (0.006) (N = 18)	0.08 (0.018) (N = 2)	0.20	0.07 (0.006) (N = 16)	0.07 (0.01) (N = 4)	0.21
TMS, EMM (SE)							
rMT, %MO (N = 23)	72.2 (6.4) (N = 8)	62.9 (4.6) (N = 15)	–	0.26	66.0 (5.4) (N = 12)	54.9 (8.8) (N = 3)	0.31
CSP, ms (N = 21)	221.7 (16.7) (N = 6)	198.4 (12.4) (N = 15)	–	0.39	175.6 (12.6) (N = 11)	241.9 (17.3) (N = 4)	0.10
LICI, log (MEPt/MEPc) (N = 18)	− 0.02 (0.27) (N = 6)	− 0.01 (0.18) (N = 12)	–	0.97	− 0.03 (0.22) (N = 10)	0.24 (0.37) (N = 2)	0.99

Individuals with no SSADH protein are compared to A) those with Single Homotetramers and Multiple Homo and Heterotetramers and B) those with different effects of protein impairments

ADOS-2 Autism Diagnostic Observation Schedule-Second Edition, *ASD* Autism Spectrum Disorder, *CSP* cortical silent period, *EEG* electroencephalogram, *EEM* estimated marginal means adjusted for age, *FSIQ* full scale intellectual quotient, *GABA* γ-aminobutyrate, *GHB* γ-hydroxybutyrate, *GBA* guanidinobutyrate, *IQR* interquartile ratio, *LICI* long interval intracortical inhibition, *MEPc* motor evoked potential, condition, *MEPt* motor evoked potential, test, *MO* machine output, *MRS* magnetic resonance spectroscopy, *ms* milliseconds, *NAA* N-acetyl aspartate, *NAD-SD* standard deviation, *SE* standard error, *SSADHD* succinic semialdehyde dehydrogenase deficiency, *TMS* transcranial magnetic stimulation, *Bold* indicates significant

*The 'No Protein' group participates in two comparisons presented in this table: (1) with the 'Single Homotetramers' and 'Multiple Homo and Heterotetramers' groups; (2) with the two "Effect in impairment" groups

**These p values represent the comparison between the groups 'No protein,' 'Single Homotetramers,' and 'Multiple Homo and Heterotetramers'

**These p values represent the comparison between the groups 'No Protein,' 'Impairment effect in Folding/Stability/Oligomerization,' and 'Impairment Effect in Catalysis'

nonsense variant and one had a splice site variant). There were no individuals in this subgroup with multiple homo or heterotetrameric proteins. Three out of the four (75%) missense variants of this subgroup were c.803G>A, p.G268E, and the other one was c.1005C>A, p.N335K (Fig. 3).

Compared to the rest of the study group, the 14 individuals with splice-site variants (12 of whom were compound heterozygotes) had significantly lower scores of the total CSS (mean ± SD of 15.5 ± 2.9 vs. 17.8 ± 2.5, $p = 0.01$) and CSS psychiatric domain (mean ± SD of 2.6 ± 1.2 vs. 3.4 ± 1.7, $p = 0.04$). These groups had no differences in other demographic, clinical, biochemical, neuroimaging, or neurophysiologic parameters. Interestingly, the single splice-site variant with Δ score < 0.5 was found in two participants with contrasting clinical courses. The first one (patient # 19), with a milder clinical outcome, had an additional missense variant (c.278G>T), resulting in milder impairments of the protein's stability and folding. The second one (patient # 59), who had a severe clinical picture including drug-resistant seizures, had an additional non-sense mutation (c.1234C>T) resulting in a truncated protein.

Discussion

SSADHD is a unique inherited disorder of GABA metabolism characterized by a particular phenotype that varies in severity. Results to date of clinical assessments and

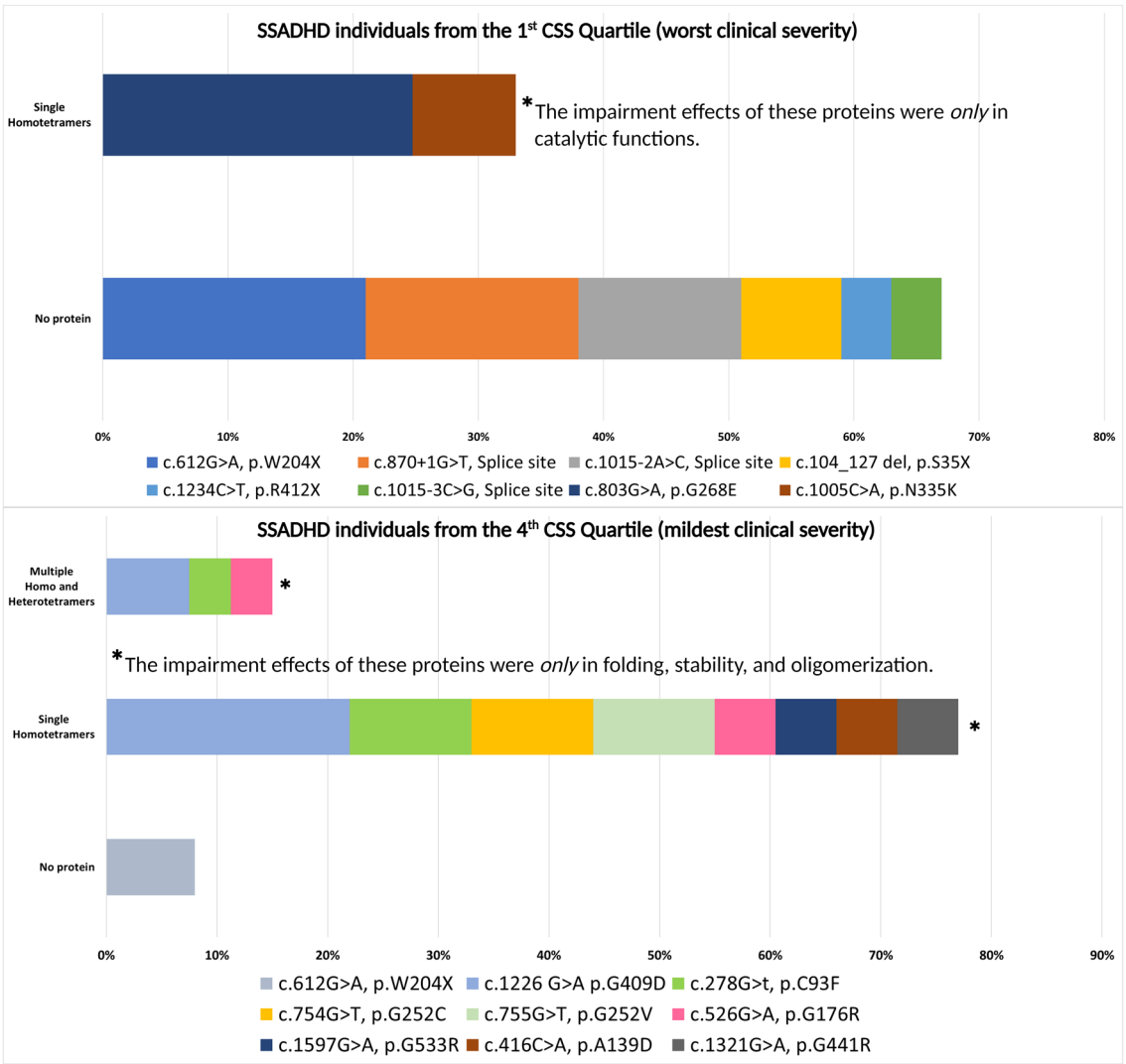

Fig. 3 Comparison of the structural and functional impairment of SSADH proteins and their associated variants of SSADHD subjects in the 1st quartile (worst severity, above) vs. 4th quartile (mildest severity, below) of the SSADHD clinical severity score (CSS)

diagnostic procedures in the ongoing SSADHD Natural History Study are adding to our growing insights into the pathophysiology of the disorder (Tokatly Latzer et al. 2023a, b, c). This study describes the first report of a genotype–phenotype correlation of SSADHD, performed on the largest studied cohort of individuals with this condition. Predictions of a genotype–phenotype correlation in monogenic diseases [e.g., phenylketonuria (Garbade et al. 2019)] are typically performed by associating genetic variants to their frequency in alleles and genotypes and finally to phenotypes. In this study, in addition to the in silico analyses we performed on individual variants, we assessed the relationship between the SSADH protein population synthesized by each subject to the molecular effect derived from the combination of their variants. Our bioinformatic analyses revealed that *ALDH5A1* variants resulting in a truncated or lack of SSADH protein, as opposed to having single homotetramers or a mixed population homo and heterotetramers, are associated with worse clinical severity. Additionally, severe clinical outcomes in SSADHD coincided with impairment in the SSADH catalytic sites, as opposed to impairments in its folding, stability, or oligomerization. Considering SSADHD is an autosomal recessive inherited condition and SSADH is an oligomeric protein, knowledge of the *ALDH5A1* allelic variants is informative only if their resultant global molecular effect on the SSADH protein is elucidated. Hence, we propose that the genetic assessments of SSADHD individuals should be protein-focused.

This study's findings determined that the 32 allelic variants (eight of which are novel), present in 41 unique allelic combinations (Table 1) in 58 SSADHD participants, were pathogenic. Considering the autosomal recessive inheritance

of SSADHD, the consequences of these variants on the phenotype of the disease cannot be explained or attributed to a single allelic variant, irrespective of its type (missense, nonsense, frame-shift, or splice site). The complexity of the genotypic profile of our study population prompted us to perform an in-depth analysis of the effect of every single variant on SSADH protein structure and function and estimate the resultant effect of the combination of variants for each study participant. This innovative approach using extensive cross-examination between genotype, synthesized protein, and phenotype has yielded new correlations and may serve as a model for other rare diseases of similar inheritance.

The information gathered from our extensive variant analysis was used to predict disease presentation using the sizeable clinical database of our natural history study. Specifically, and in contrast with other studies which were limited in their assessment of the genotype–phenotype relationship by a lack of well-characterized phenotypical information (Akaboshi et al. 2003; DiBacco et al. 2020; Pop et al. 2020), the clinical phenotype of our patients was thoroughly characterized with a validated clinical severity score along with several quantitative clinical and neurometabolic parameters. This allowed us to more precisely assess the impact of the predicted protein number and functionality on disease outcomes.

A major outcome of the study is the finding that having variant combinations resulting in no SSADH protein or a truncated enzyme predicted worse overall clinical severity, worse cognitive abilities, worse psychiatric symptomatology, and increased seizure intensity. Additionally, we saw that variants resulting in multiple homo or heterotetrameric proteins were associated with fewer seizures and dyskinetic movement disorders than variants resulting in no protein or single homotetrameric proteins. This could be due to positive complementation effects resulting from the combination of polypeptide chains in the SSADH tetramer or from mRNA interallelic splicing that restores one healthy wild-type polypeptide chain. Comparison of the mutated protein structures and functions in subjects whose CSS fell in the 1st and 4th CSS quartiles further supported these observations. Most subjects from the 1st (worst severity) quartile had no protein, and none had multiple homo and heterotetrameric proteins. In contrast, only one subject from the 4th (mildest severity) CSS quartile had no protein. Why a lack of the SSADH enzyme coincides with the worst clinical outcome as compared to having single homotetrameric or multiple homo and heterotetrameric SSADH proteins can be intuitive, based on the fact that even malfunctioning enzyme variants can provide a minimum of catalytic activity. Moreover, the functional or partly functional SSADH protein has a tetrameric assembly. In compound heterozygous SSADHD subjects, this may lead to a possibility of many polypeptide chain combinations resulting in different clinical phenotypes. This phenomenon is also observed in other inherited metabolic disorders; in aromatic L-amino acid decarboxylase (AADC) deficiency, a splicing mutation leading to the absence of the enzyme is associated with the most severe clinical phenotype (Wassenberg et al. 2017). In phenylketonuria, splicing mutations are predicted to affect protein synthesis critically and worsen clinical outcomes. Further, in compound heterozygous phenylketonuria patients, variable production of phenylalanine and degrees of clinical severity depend on the combined effect of their two variants (Jin et al. 2022).

As expected, the expression of *ALDH5A1* was also lower in subjects who completely lacked the protein. Conceptually, it would be anticipated that a complete lack of the SSADH enzyme would result in higher values of cerebral and systemic GABA and its metabolites and accordingly, in cortical inhibition. However, no differences were found between protein subgroups in the age-adjusted means of MRS-derived GABA/NAA ratio, plasma GABA, GHB, and GBA levels, and TMS-derived indices of cortical inhibition. This could result from the small sample size of these subgroups or the absence of MRS and TMS data in the multiple homo and heterotetrameric proteins subgroup. It is also possible that this lack of correlation resulted from other multifactorial influences and complex GABAergic homeostatic mechanisms affecting the concentrations of GABA and its metabolites. GABA (and GABA-related metabolites) were shown to be dependent on GABA receptor expression (known to be downregulated in SSADHD) (Lee et al. 2022; Reis et al. 2012; Pearl et al. 2009) and polymorphisms in genes related to the GABA shunt (Akaboshi et al. 2003). Longitudinal measurement of these neurotransmitters will be needed to estimate the trajectory of their concentrations in relation to genotype.

Another significant outcome of the study is that subjects whose variants result in proteins impaired in stability, folding, or oligomerization have better overall clinical outcomes and adaptive functions than those with no protein or protein with impaired catalytic function. Here again, comparisons of subjects' protein structural and functional profiles in the 1st and 4th quartiles of clinical severity scores were informative. The type of protein impairment observed in patients within the 1st CSS quartile (worst severity) was limited to impairment in catalytic function, as opposed to all subjects in the 4th quartile who only had single homotetrameric or homo and heterotetrameric proteins impaired in stability, folding, or oligomerization. In other inherited metabolic disorders, it has been reported that defects in folding, stability, or oligomerization are less disruptive than those resulting in loss of function from catalytic defects. In AADC deficiency, for example, purified recombinant pathogenic variants prone to misfolding or aggregation were shown to maintain catalytic

activity, contributing to milder clinical phenotypes. In contrast, variants resulting in catalytic impairments usually lead to loss of function despite the lack of their structural disassembly (Montioli et al. 2020). Another example may be provided from phenylketonuria, in which it was demonstrated that residual activity of phenylalanine hydroxylase is the major determinant for disease severity in functionally hemizygous patients (Himmelreich et al. 2018). While folding and stability defects affect the oligomeric equilibrium between tetrameric and dimeric species of phenylalanine hydroxylase, they are related to milder forms of the disease (Erlandsen and Stevens 2001). The explanation for these findings could also stem from evidence demonstrating that the catalytic loop of the enzyme is influenced by environmental redox status, which in turn can lead to its structural modifications (Kim et al. 2009). Two cysteine residues mapping on that catalytic loop regulate this process: Cys340 and Cys342. Amino acid substitutions altering the mobility of the 2-Cys loop may negatively affect the proper response to reactive oxygen species and change in redox status. Among the identified *ALDH5A1* variants, N335K and G441R are in proximity to the 2-Cys loop and could be responsible for the worst phenotypes characterizing functionally hemizygous SSADHD subjects bearing them. One further issue that may be raised with respect to the similar outcomes and associations of the subgroups of subjects with no protein and those with a catalytic defect relates to whether the metabolic consequences of low availability of NAD^+ leads to reduced function of the enzyme. Future analyses may quantitate NAD^+ binding to assess whether loss or reduction of catalytic activity can be differentiated by metabolic changes and corresponding levels of phenotypic severity.

Our findings also have implications for gene replacement therapy for SSADHD. Since a functional SSADH is arranged in a tetrameric form, the proper assembly of the enzyme after gene therapy may ultimately govern therapeutic outcomes and efficacy. It is generally accepted that SSADH variant carriers are non-symptomatic. However, reports have suggested that non-pathogenic SSADH polymorphism leading to ~ 82% enzyme activity might suffice to contribute to cognitive decline and reduced survival in the elderly (Rango et al. 2008). The knowledge gained from our structural and functional analyses of pathogenic *ALDH5A1* variants may thus be useful in the design of gene-editing or gene-replacement strategies, helping predict the functionality of the monomers produced by the wild-type gene when they assemble with the patients' diseased monomers, and optimize the utility of gene therapy.

There are limitations to our study. While the genetic and protein analyses we performed are from the largest cohort of SSADHD patients ever studied, not all participants underwent all the neuroimaging, neurophysiologic, and neuropsychiatric assessments. This limitation is common in rare disease research, especially when affected individuals have a low tolerance to lengthy study procedures without sedation. Further, it must be pointed out that the bioinformatic predictions of SSADH structure and function are based on the enzyme's crystal structure. Crystal structures are "frozen" models that cannot be used to predict the structural mobility of enzymes in their active state. In the case of SSADH, working with the crystal structure of the protein may have led to underestimating the impact of some variants on the catalytic capacity of the enzyme and disease presentation. Future studies will be needed to address this point, where recombinant SSADH variants will be cloned and expressed in appropriate cell models in combinations matching those of the individuals enrolled in our natural history study. These in vitro models would then be used to perform "personalized" predictions between the variant profile of each patient, enzyme kinetics parameters, and the patient's clinical presentation. Lastly, as discussed above, other genetic factors likely contribute to disease presentation. These factors include the patient's family genetic background, genes involved in the expression of GABA receptors, and receptors known to regulate downstream GABA signaling pathways. The expression of GABA receptors (their subunits) was not assayed in our study samples but should be included in customized profiler arrays in the future. Such information would complete the neurobiological interpretation of our findings related to the regulatory changes of GABA receptors in response to the hyperGABAergic state of the patients.

Conclusions

This is the first comprehensive study of genotype-to-protein-to-phenotype correlations in SSADHD, an autosomal recessive inherited disorder with a unique neurometabolic phenotype. Bioinformatics and in silico modeling of a large number of *ALDH5A1* variants were used to predict the impact of the variants and variant combinations on protein structure and function. This information, coupled with the extensive clinical information gathered from the SSADHD natural history study, provided significant and novel insights into the relationships between gene, gene product, and disease phenotype. Worse clinical outcome was found in SSADHD subjects with a resultant lack of protein, as opposed to single homotetramers or multiple homo and heterotetramers. A milder clinical severity was seen in those whose resultant proteins were impaired in their stability, folding, or oligomerization as opposed to catalytic sites or lacking a protein. These findings are clinically relevant and potentially useful for prognostic estimations, disease management, and patient selection in future gene replacement therapy trials. Importantly, our approach to studying a genotype–phenotype relationship, including protein structure and

function, may serve as a template to determine genotype-to-protein-to-phenotype relationships in other autosomal recessive rare disorders.

Acknowledgements We are grateful to the individuals with SSADHD and their families who agreed to participate in this study and for the ongoing support of the SSADHD Association (http://www.ssadh.net).

Author contributions All authors contributed to the study conception and design. Material preparation, data collection and analysis were performed by ITL, J-BR, MB, SC, MLD, EA, AR, HHCL, TO, KJ, ÀG-C, NJ-P, KMG, and PP. The first draft of the manuscript was written by ITL and all authors commented on previous versions of the manuscript. All authors read and approved the final manuscript.

Funding Funding for the SSADHD Natural History study is provided by the National Institutes of Health (1R01HD091142).

Data availability The datasets generated during and/or analyzed during the current study are available from the corresponding author on reasonable request.

Declarations

Conflict of interest The authors I.T.L, J.B.R., M.B., S.C., M.L.D., E.A., T.O., K.J., À.G.C., N.J.P., K.M.G. have no relevant financial or non-financial interests to discolose. The authors A.R. and H.H.C.L. are co-founders and have equity in Galibra Neuroscience, Inc., which develops treatments for SSADH deficiency, including gene replacement therapy mentioned in this study. The authors A.R., H.C.C.L., and P.L.P. are inventors of a filed SSADH deficiency gene therapy patent.

Ethics approval This study was performed in line with the principles of the Declaration of Helsinki. Approval was granted by the Institutional Review Board of Boston Children's Hospital (#P00029917).

Consent to participate Written informed consent was obtained from all individual participants or their parents/legal guardians included in the study.

Consent to publish individual personal data N/A.

References

Achenbach TM, Rescorla LA (2000) Child behavior checklist for ages 1 1/2-5: ASEBA. University of Vermont, Burlington

Achenbach TM, Rescorla LA (2001) Manual for the ASEBA school-age forms & profiles: an integrated system of multi-informant assessment. University of Vermont, Research Center for Children, Youth, & Families, Burlington, p 1617

Achenbach TM, Rescorla L (2003) ASEBA adult forms & profiles: for ages 18–59: adult self-report and adult behavior checklist. Aseba, Burlington

Afacan O, Yang E, Lin AP et al (2021) Magnetic resonance imaging (MRI) and spectroscopy in succinic semialdehyde dehydrogenase deficiency. J Child Neurol 36(13–14):1162–1168

Akaboshi S, Hogema BM, Novelletto A et al (2003a) Mutational spectrum of the succinate semialdehyde dehydrogenase (ALDH5A1) gene and functional analysis of 27 novel disease-causing mutations in patients with SSADH deficiency. Hum Mutat 22(6):442–450

Arning E, Wasek B, Bottiglieri T (2022) Quantitation of γ-aminobutyric acid in cerebrospinal fluid using liquid chromatography-electrospray-tandem mass spectrometry. Clinical applications of mass spectrometry in biomolecular analysis. Springer, Berlin, pp 165–174

Attri SV, Singhi P, Wiwattanadittakul N et al (2017) Incidence and geographic distribution of succinic semialdehyde dehydrogenase (SSADH) deficiency. JIMD Rep 34:111–115

Bisello G, Bertoldi M (2022) Compound heterozygosis in AADC deficiency and its complex phenotype in terms of AADC protein population. Int J Mol Sci 23(19):11238

Bzoch KR, League R, Brown V (2003) REEL 3: receptive-expressive emergent language test. Pro-Ed

Chambliss KL, Caudle DL, Hinson DD et al (1995) Molecular cloning of the mature NAD(+)-dependent succinic semialdehyde dehydrogenase from rat and human. cDNA isolation, evolutionary homology, and tissue expression. J Biol Chem 270(1):461–467

Costigan AG, Umla-Runge K, Evans CJ et al (2019) Neurochemical correlates of scene processing in the precuneus/posterior cingulate cortex: a multimodal fMRI and 1H-MRS study. Hum Brain Mapp 40(10):2884–2898

De Rango F, Leone O, Dato S et al (2008) Cognitive functioning and survival in the elderly: the SSADH C538T polymorphism. Ann Hum Genet 72(Pt 5):630–635

DiBacco ML, Pop A, Salomons GS et al (2020a) Novel ALDH5A1 variants and genotype: phenotype correlation in SSADH deficiency. Neurology 95(19):e2675–e2682

Duncan NW, Zhang J, Northoff G et al (2019) Investigating GABA concentrations measured with macromolecule suppressed and unsuppressed MEGA-PRESS MR spectroscopy and their relationship with BOLD responses in the occipital cortex. J Magn Reson Imaging 50(4):1285–1294

Beran TN, Elliott CD (2007) Differential ability scales, 2nd ed. Harcourt Assessment, San Antonio. Can J School Psychol 22:128–32

Erlandsen H, Stevens RC (2001) A structural hypothesis for BH4 responsiveness in patients with mild forms of hyperphenylalaninaemia and phenylketonuria. J Inherit Metab Dis 24(2):213–230

Garbade SF, Shen N, Himmelreich N et al (2019) Allelic phenotype values: a model for genotype-based phenotype prediction in phenylketonuria. Genet Med 21(3):580–590

Henderson SE, Sugden D, Barnett AL (2007) Movement assessment battery for children-2. APA Psyc Tests. https://doi.org/10.1037/t55281-000

Himmelreich N, Shen N, Okun JG et al (2018) Relationship between genotype, phenylalanine hydroxylase expression and in vitro activity and metabolic phenotype in phenylketonuria. Mol Genet Metab 125(1–2):86–95

Hogema BM, Gupta M, Senephansiri H et al (2001) Pharmacologic rescue of lethal seizures in mice deficient in succinate semialdehyde dehydrogenase. Nat Genet 29(2):212–216

Institute B (2023) SpliceAI Lookup. https://spliceailookup.broadinstitute.org/. Accessed June 2023

Jaganathan K, Panagiotopoulou SK, McRae JF et al (2019) Predicting splicing from primary sequence with deep learning. Cell 176(3):535–548 (**e24**)

Jansen EE, Struys E, Jakobs C et al (2008) Neurotransmitter alterations in embryonic succinate semialdehyde dehydrogenase (SSADH) deficiency suggest a heightened excitatory state during development. BMC Dev Biol 8:112

Jin X, Yan Y, Zhang C et al (2022) Identification of novel deep intronic PAH gene variants in patients diagnosed with phenylketonuria. Hum Mutat 43(1):56–66

Kim YG, Lee S, Kwon OS et al (2009a) Redox-switch modulation of human SSADH by dynamic catalytic loop. EMBO J 28(7):959–968

Kwan P, Arzimanoglou A, Berg AT et al (2010) Definition of drug resistant epilepsy: consensus proposal by the ad hoc Task Force of the ILAE Commission on Therapeutic Strategies. Epilepsia 51(6):1069–1077
Lee HHC, Pearl PL, Rotenberg A (2021) Enzyme replacement therapy for succinic semialdehyde dehydrogenase deficiency: relevance in γ-aminobutyric acid plasticity. J Child Neurol 36(13–14):1200–1209
Lee HHC, McGinty GE, Pearl PL et al (2022) Understanding the molecular mechanisms of succinic semialdehyde dehydrogenase deficiency (SSADHD): towards the development of SSADH-targeted medicine. Int J Mol Sci 23(5):2606
Lord C, Rutter M, DiLavore P et al (2012) Autism diagnostic observation schedule, (ADOS-2). Western Psychological Services, Torrance
Martin K, McConnell A, Elsea SH (2021) Assessing prevalence and carrier frequency of succinic semialdehyde dehydrogenase deficiency. J Child Neurol 36(13–14):1218–1222
Montioli R, Bisello G, Dindo M et al (2020) New variants of AADC deficiency expand the knowledge of enzymatic phenotypes. Arch Biochem Biophys 682:108263
Mullen EM (1995) Mullen scales of early learning. AGS, Circle Pines
Ogino S, Gulley ML, den Dunnen JT et al (2007) Standard mutation nomenclature in molecular diagnostics: practical and educational challenges. J Mol Diagn 9(1):1–6
Parthiban V, Gromiha MM, Schomburg D (2006) CUPSAT: prediction of protein stability upon point mutations. Nucleic Acids Res 34(1):W239–W242
Pearl PL, Gibson KM, Acosta MT et al (2003) Clinical spectrum of succinic semialdehyde dehydrogenase deficiency. Neurology 60(9):1413–1417
Pearl PL, Gibson KM, Quezado Z et al (2009) Decreased GABA-A binding on FMZ-PET in succinic semialdehyde dehydrogenase deficiency. Neurology 73(6):423–429
Pearl PL, Parviz M, Vogel K et al (2015) Inherited disorders of gamma-aminobutyric acid metabolism and advances in ALDH5A1 mutation identification. Dev Med Child Neurol 57(7):611–617
Peek A, Rebbeck T, Leaver A et al (2021) A comprehensive guide to mega-press for Gaba measurement. medRxiv 7:35
Pop A, Smith DEC, Kirby T et al (2020) Functional analysis of thirty-four suspected pathogenic missense variants in ALDH5A1 gene associated with succinic semialdehyde dehydrogenase deficiency. Mol Genet Metab 130(3):172–178
Provencher SW (2021) LCModel & LCMGUI user's manual version 6.3–1R. [February 2023]. http://s-provencher.com/pub/LCModel/manual/manual.pdf. Accessed June 2023
Reis J, Cohen LG, Pearl PL et al (2012) GABAB-ergic motor cortex dysfunction in SSADH deficiency. Neurology 79(1):47–54
Richards S, Aziz N, Bale S et al (2015) Standards and guidelines for the interpretation of sequence variants: a joint consensus recommendation of the American College of Medical Genetics and Genomics and the Association for Molecular Pathology. Genet Med 17(5):405–424
Sehnal D, Bittrich S, Deshpande M et al (2021) Mol* Viewer: modern web app for 3D visualization and analysis of large biomolecular structures. Nucleic Acids Res 49(W1):W431–W437
Sparrow SS, Cicchetti DV, Balla DA (2005) Vineland adaptive behavior scales (VABS). NCS Pearson, Bloomington
Tokatly Latzer I, Roullet JB, Gibson KM et al (2023a) Establishment and validation of a clinical severity scoring system for succinic semialdehyde dehydrogenase deficiency. J Inherit Metab Dis 46:992
Tokatly Latzer I, Hanson E, Bertoldi M et al (2023b) Autism spectrum disorder and GABA levels in children with succinic semialdehyde dehydrogenase deficiency. Dev Med Child Neurol 65:1596
Tokatly Latzer I, Bertoldi M, DiBacco ML et al (2023c) The presence and severity of epilepsy coincide with reduced γ-aminobutyrate and cortical excitatory markers in succinic semialdehyde dehydrogenase deficiency. Epilepsia 64:1516
Tsuboyama M, Kaye HL, Rotenberg A (2020) Review of transcranial magnetic stimulation in epilepsy. Clin Ther 42(7):1155–1168
Wassenberg T, Molero-Luis M, Jeltsch K et al (2017) Consensus guideline for the diagnosis and treatment of aromatic l-amino acid decarboxylase (AADC) deficiency. Orphanet J Rare Dis 12(1):12
Wechsler D (1999) Wechsler Abbreviated Scale of Intelligence (WASI). APA Psyc Tests. https://doi.org/10.1037/t15170-000
Yamakawa Y, Nakazawa T, Ishida A et al (2012) A boy with a severe phenotype of succinic semialdehyde dehydrogenase deficiency. Brain Dev 34(2):107–112

Authors and Affiliations

Itay Tokatly Latzer[1,2] · Jean-Baptiste Roullet[3] · Samuele Cesaro[4] · Melissa L. DiBacco[1] · Erland Arning[5] · Alexander Rotenberg[1,6] · Henry H. C. Lee[6,7] · Thomas Opladen[8] · Kathrin Jeltsch[8] · Àngels García-Cazorla[9] · Natalia Juliá-Palacios[9] · K. Michael Gibson[3] · Mariarita Bertoldi[4] · Phillip L. Pearl[1]

✉ Mariarita Bertoldi
mita.bertoldi@univr.it

✉ Phillip L. Pearl
Phillip.Pearl@childrens.harvard.edu

Itay Tokatly Latzer
itay.tokatlylatzer@childrens.harvard.edu

Jean-Baptiste Roullet
j.roullet@wsu.edu

Samuele Cesaro
samuele.cesaro@univr.it

Melissa L. DiBacco
Melissa.DiBacco@childrens.harvard.edu

Erland Arning
Erland.Arning@BSWHealth.org

Alexander Rotenberg
alexander.rotenberg@childrens.harvard.edu

Henry H. C. Lee
hingcheong.lee@childrens.harvard.edu

Thomas Opladen
Thomas.Opladen@med.uni-heidelberg.de

Kathrin Jeltsch
Kathrin.Jeltsch@med.uni-heidelberg.de

Àngels García-Cazorla
agarcia@sjdhospitalbarcelona.org

Natalia Juliá-Palacios
nataliaalexandra.julia@sjd.es

K. Michael Gibson
mike.gibson@wsu.edu

[1] Department of Neurology, Boston Children's Hospital, Harvard Medical School, 300 Longwood Ave, Boston, MA 02115, USA

[2] Faculty of Medicine, Tel-Aviv University, Tel Aviv, Israel

[3] Department of Pharmacotherapy, College of Pharmacy and Pharmaceutical Sciences, Washington State University, Spokane, WA, USA

[4] Department of Neuroscience, Biomedicine and Movement Sciences, University of Verona, Strada Le Grazie 8, 37134 Verona, VR, Italy

[5] Institute of Metabolic Disease, Baylor Scott & White Research Institute, Dallas, TX, USA

[6] F.M. Kirby Neurobiology Center, Boston Children's Hospital, Boston, MA 02115, USA

[7] Rosamund Stone Zander Translational Neuroscience Center, Boston Children's Hospital, Boston, MA 02115, USA

[8] Division of Neuropediatrics and Metabolic Medicine, University Children's Hospital Heidelberg, Im Neuenheimer Feld 430, 69120 Heidelberg, Germany

[9] Neurometabolic Unit, Neurology Department, Institut de Recerca, Hospital Sant Joan de Déu, Barcelona, Spain